

## Friction Behavior of TiAlN, AlTiN and AlCrN Multilayer Coatings at Nanoscale

Doğuş ÖZKAN

National Defense University, Naval Academy, Mechanical Engineering Department, Tuzla, Istanbul, Turkey

Geliş / Received:04/06/2018, Kabul / Accepted: 21/11/2018

### Abstract

In this study, 3.5 µm thick TiAlN, AlTiN, and AlCrN multilayer coatings were deposited on the H13 steel surface by physical vapor deposition (PVD) method. Friction behavior of these coatings was investigated by friction force microscopy for the first time at nanoscale in the literature. Friction force measurements were performed with the atomic force microscopy lateral force mode at various loads. Results showed that the AlTiN coating had three times lower COF value than the TiAlN and AlCrN coatings due to the lower surface energy. It was observed in this study that Amonton's law was valid for the COF evolution at the nanoscale.

**Keywords:** Amonton's Law, Elastic Modulus, Friction Force Microscopy, Physical Vapor Deposition (Pvd), Surface Energy

### Çok Katmanlı TiAlN, AlTiN ve AlCrN Kaplamaların Nanoboyuttaki Sürtünme Davranışları

#### Öz

Bu çalışmada H13 çeliği üzerine fiziksel buharlaştırma yöntemi ile 3.5 mikron kalınlığa sahip çok katmanlı TiAlN, AlTiN ve AlCrN kaplamalar yapılmıştır. Kaplamaların sürtünme karakteristikleri sürtünme kuvveti mikroskopisi ile nano mertebede literatürde ilk kez araştırılmıştır. Sürtünme kuvveti ölçümleri değişen yükler altında atomik kuvvet mikroskopunun yatay kuvvet modunda gerçekleştirilmiştir. Sonuçlar AlTiN kaplamasının diğer kaplamalara göre düşük yüzey enerjisi nedeni ile üç kat daha az sürtünme katsayısına sahip olduğunu göstermiştir. Bu çalışmada Amonton yasasının nano mertebede sürtünme katsayısını bulmada geçerli olduğu gözlemlenmiştir.

**Anahtar Kelimeler:** Amonton Yasası, Elastik Modülü, Fiziksel Buharlaştırma ile Biriktirme, Sürtünme Kuvveti Mikroskopisi, Yüzey Enerjisi

## 1. Introduction

Friction is an important phenomenon due to the energy loss and material damage in tribological systems (Bhushan, 1999). Therefore, it is essential to control and reduce friction between sliding surfaces (Stachowiak and Batchelor, 2000). Especially, friction is the source of 33% the mechanical loss in internal combustion engines (Chu and Majumdar, 2012; Holmberg et al., 2012) and friction should be decreased in moving parts of the engine for fuel saving in consideration of global energy conservation (Rosen et al., 1996). One way to overcome energy loss caused by friction is surface coatings, which provide lower

friction coefficient (COF) between sliding surfaces (Sang et al., 2008). Therefore, various surface treatments are applied to some moving parts of engines. For instance, piston rings are generally coated with chromium to get low friction and wear resistance. Similarly, crank bearings are coated with different composites such as aluminum alloy, and copper-lead-tin alloys (Badisch and Roy, 2013; Lauda, 2007). Friction Force Microscopy (FFM) by Atomic Force Microscope (AFM) can evaluate friction force measurements. The frictional force on the conic tip or colloidal probe is measured while sliding on a surface at a constant velocity at the nanoscale (Holscher et al., 2008; Ruan and Bhushan, 1993). force

on the conic tip or colloidal probe is measured while sliding on a surface at a constant velocity at the nanoscale (Holscher et al., 2008; Ruan and Bhushan, 1993). A literature survey showed that friction force depends on surface roughness, sliding speed, sliding distance and applied normal load (Zhang and Lan, 2002; Manini et al., 2017; Svahn et al., 2003). In this study, friction coefficients of TiAlN, AlTiN and AlCrN thin film coatings were evaluated by friction force microscopy (FFM). According to the literature survey, the friction of these coatings has been evaluated by dry sliding tribometer tests at the macro scale. Mo and Zhu investigated the tribological behavior of CrN, AlCrN and TiAlN PVD deposited coatings at 5 N load with dry sliding tribometer tests (Mo et al., 2007; Mo and Zhu, 2009). Liew et al. investigated frictional and wear behavior of single layer and multilayer AlCrN, TiAlN, TiN and AlN coatings with tribometer tests at 5 N load under dry condition (Liew et al., 2013). However, friction behavior of these coatings in the literature has not yet been investigated at the nanoscale. This study aims to investigate friction behavior TiAlN, AlTiN and AlCrN thin film coatings by FFM at the nanoscale and atomic force microscope (AFM) was used to evaluate the friction

behavior of the coatings with lateral force mode. Results showed that AlTiN had lower COF than TiAlN and AlCrN coatings due to its lower level of surface energy.

## 2. Material and Method

### 2.1. Coating Method and Characterization of The Coatings

H13 steel samples were used as a substrate and its typical chemical composition is given in Table-1. Substrates were mechanically polished to an average surface roughness of 150  $\mu\text{m}$ , and then ultrasonically cleaned for nitrating operation. 3.5  $\mu\text{m}$  thick multilayer TiAlN, AlTiN and AlCrN coatings were deposited on steel substrates by Cathodic Arc Physical Vapor Deposition (CAPVD) coating method. Al67Ti33 and Al70Cr33 targets were used to deposit TiAlN, AlTiN and AlCrN coatings, respectively. Prior to the deposition process, H13 tool steel samples were first heated to 450°C, then ion etched via Cr bombardment. During the coating process, the temperature of the substrate was kept at about 450 °C due to the IR and plasma heating. In addition, vacuum pressure level of the chamber was about  $10^{-3}$  Pa. The nitrating process was carried under 100 V bias voltage and 99.9 % Nitrogen purity at 1 Pa pressure.

**Table 1.** The chemical composition of the H13 steel. Element Content % in weight.

Element Content % in weight									
Cr	Mo	Si	V	C	Ni	Cu	Mn	P	S
4.80	1.15	0.92	0.88	0.38	0.3	0.24	0.35	0.03	0.03

After the coating process, substrate surfaces were investigated by SEM/EDX and XRD analysis to characterize the coatings. Hardness and elastic modulus of the coatings were evaluated by Nanoindenter analysis.

### 2.2. Friction Force Microscopy Measurements

Nanosurf Flex-5 AFM was used for FFM measurements. Nanosensors LFMR  $\text{Si}_3\text{N}_4$  rectangular Cantilever (length=225  $\mu\text{m}$ , width=46, tip height=12  $\mu\text{m}$ , thickness=1.6  $\mu\text{m}$ ) with 0.79 N/m nominal spring constant was used in FFM measurements. It is

essential to convert AFM friction force data measurement units from mV to nN. Therefore, Cantilever was calibrated with dimension-dependent Wedge calibration method to obtain the conversion factor ( $\alpha$ ) with the following equations. Normal Cantilever spring constant,  $k_n$  and lateral cantilever spring constant,  $k_l$  was calculated by Equation 1 and 2.

$$k_n = \frac{t^3 \cdot E \cdot w}{3 \cdot L^3} \quad (1)$$

$$k_l = \frac{G \cdot w \cdot t^3}{3 \cdot L \cdot \left(h + \frac{t}{2}\right)^2} \quad (2)$$

where, E, G, w, L, t, h are the Elastic modulus, shear modulus, width, length, the thickness of the cantilever and the tip height, respectively. Lateral deflection sensitivity of the AFM photodiode was calculated by Equation 3.  $S_n$  is the normal deflection of the photodiode, which can be obtained from the slope of the force-distance curve. Conversion factor can be found in nN/mV unit by substituting Equation 2 and 3, as shown in Equation 4.

$$S_l = \frac{E \cdot \left(h + \frac{t}{2}\right)}{2 \cdot E \cdot G} \cdot S_n \quad (3)$$

$$\alpha = S_l \cdot k_l \quad (4)$$

Friction force signal of the FFM measurement can be converted from mV to nN by using Equation (5), where  $\Delta V$  is the half of backward friction signal subtraction from the forward friction signal. Here, the calculated  $\alpha$  was 49.1 nN/mV for the LFMR rectangular Cantilever.

$$F_F = \alpha \cdot \left( \frac{V_{Fbackward} - V_{Fforward}}{2} \right) \quad (5)$$

In the friction force measurements, friction force data collection was conducted between

0 nN normal load up to 120 nN with 10 nN steps.

### 3. Result and Discussion

#### 3.1. Characterization Results of The Coatings

Figure 1 shows optical microscopy, SEM/EDX analysis results and it can be seen from the EDX spectra that desired multilayer coatings deposited on the steel surface with approximately 3.5  $\mu\text{m}$  thickness. When looking at the optical image of the AlCrN, it can be seen more coating residues on the surface when compared to TiAlN and AlTiN coatings.

CrN transition layers, which are depicted with the yellow arrows, were used to get multilayer coating. The measured hardness values of the TiAlN, AlTiN and AlCrN coatings were 29.75, 31.06, 30.72 GPa, respectively. Similar hardness values were obtained for coatings. When looking at the elastic modulus results, similar elastic modulus values were detected for AlCrN (382 GPa) and TiAlN (385 GPa) coatings. However, the elastic modulus of AlTiN (416 GPa) was higher than the other coatings. The elastic modulus of the surfaces is an important parameter since surface energy varies with a modulus of elasticity, number of surface atoms, coordination number and it can be defined by Gillman's equation (see Eq.6), where  $\gamma$  is the surface energy,  $c_0$  is the equilibrium lattice constant perpendicular to plane,  $d_0$  is the elastic distance of attractive forces acting on Cantilever. An increase in elastic modulus decreases the surface energy, which effects the shear stress of surface (Buckley, 1981; Xu et al., 2017). Surface roughness of the coatings was recorded by AFM topography image with 90x90  $\mu\text{m}^2$  scan area. Surface roughness of the coatings was recorded by the AFM topography image (see Fig. 2). The measured root mean square roughness (Rq) of the

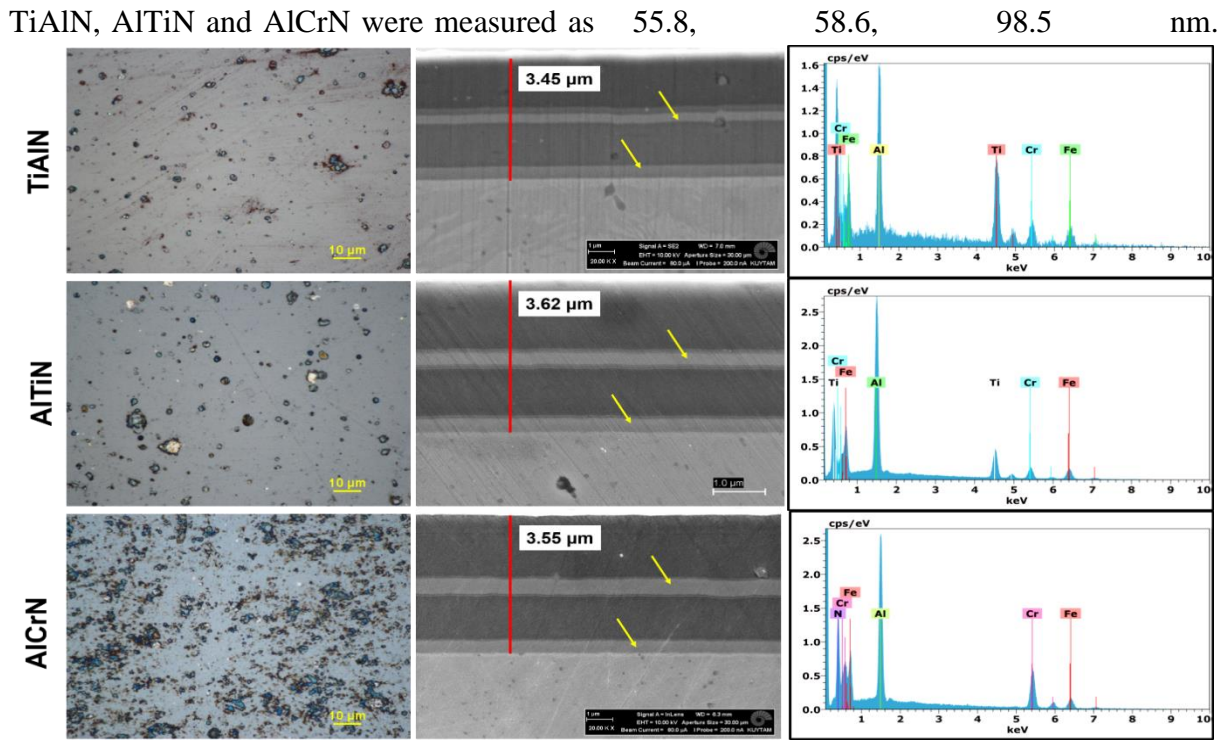


Figure 1. Optical microscopy, SEM/EDX analyses of the TiAlN, AlTiN and AlCrN coatings.

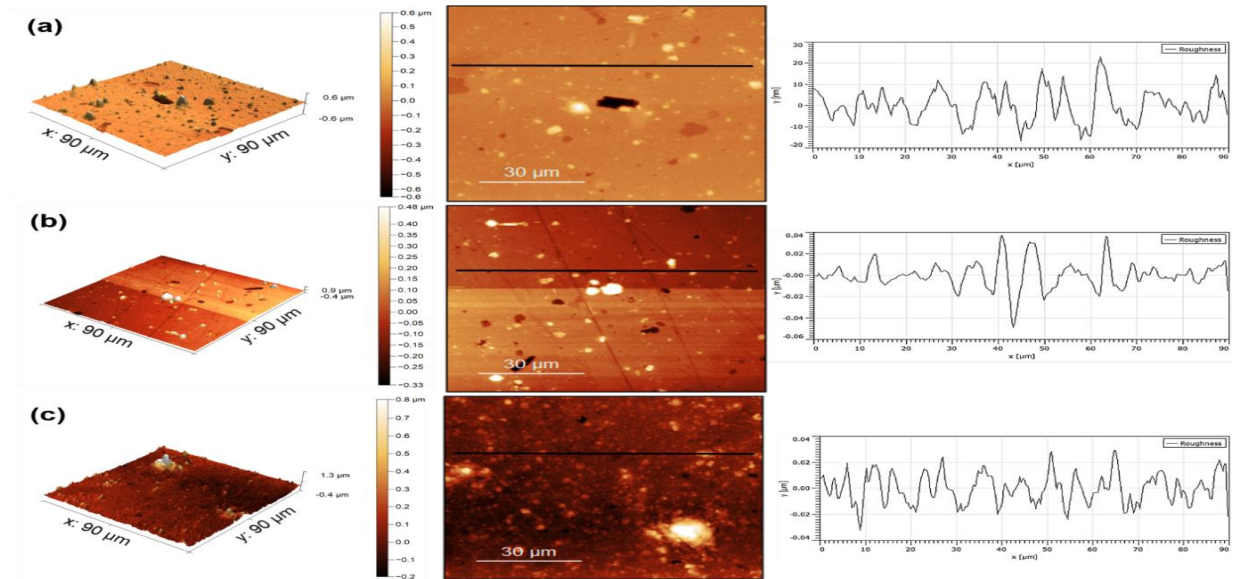


Figure 2. AFM topography images and roughness ( $R_q$ ) analysis of the (a) TiAlN, (b) AlTiN and (c) AlCrN coatings.

$$\gamma = \left(\frac{E}{c_0}\right) \cdot (d_0 - \pi)^2 \quad (6)$$

### 3.2. Friction Force Measurement Results

To check the conversion factor and FFM measurements, Si(100) surface was scanned

before starting the friction force evaluation of the TiAlN, AlTiN and AlCrN coatings. Figure 3 shows the FFM results of the Si(100) with load deviation versus friction force.

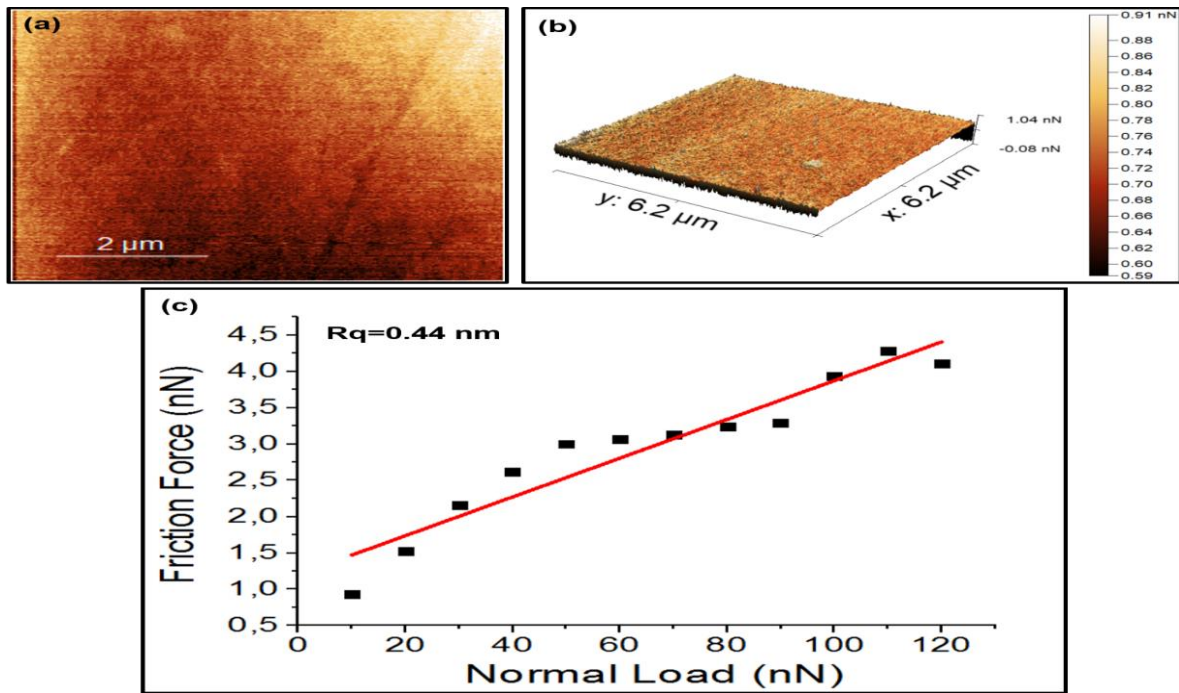


**Figure 3.** Friction force measurement results of Si(100), (a) AFM topography image of Si(100), (b) Friction force map of 10 nN load, (c) COF of Si(100) in range of 10-120 nN load.

COF evaluated by taking the slope of load-friction force curve, where 0.027 was found for Si(100) with  $R_q=0.4$  nm in this study. Bhushan et al. reported similar COF finding (0.03) for Si(111) against  $\text{Si}_3\text{N}_4$  Cantilever, which the  $R_q$  value of the sample was 0.11 (Bhushan et al., 1995). Asay et al. also reported that COF of Si sample should be in range of 0.03-0.44 (Asay and Kima, 2006). When compared to literature findings, it can be seen that our COF result was similar with literature findings, and this shows that our conversion factor was correct.

Figure 4 shows AFM friction force maps of the TiAlN, AlTiN and AlCrN coatings at 50 and 100 nN loads. Three profiles were extracted from friction force results for 10 nN load to 120 nN load and average friction force value of these profiles was plotted versus load as shown in Figure 5.

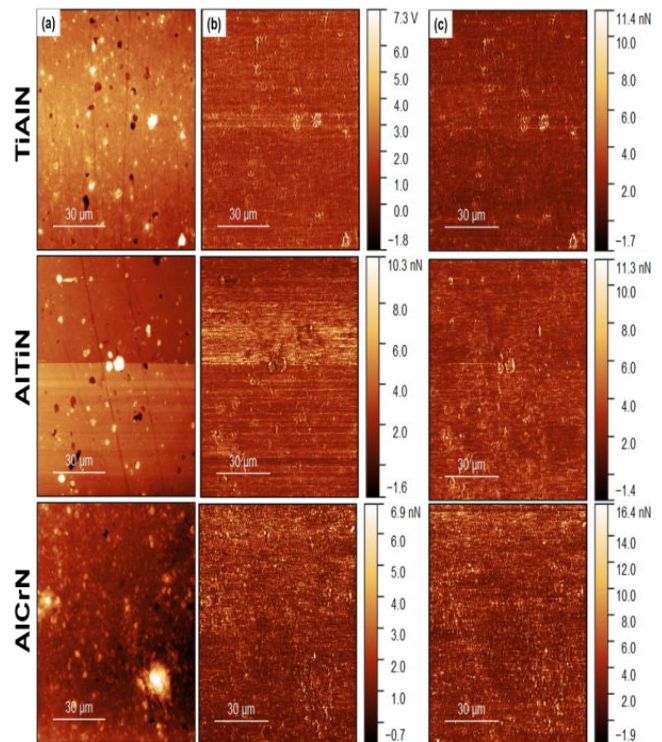


**Figure 4.** Friction force results of the TiAlN, AlTiN and AlCrN coatings, column (a) AFM topography images, column (b) friction force maps at 50 nN load, column (c) friction force maps at 100 nN load.

The slope of the friction force curves presented 0.035, 0.036 and 0.012 COF value for TiAlN, AlCrN and AlTiN coatings, respectively (see Figure 5). While TiAlN and

AlCrN showed similar COF, AlTiN showed the lowest COF. The lower COF value for AlTiN coating than the other coatings can be attributed to surface energy.

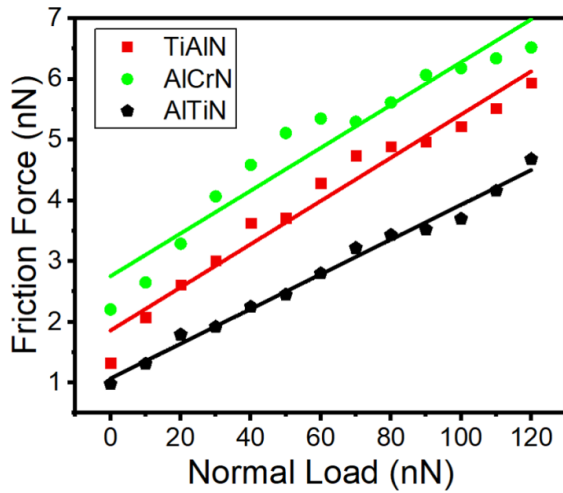


**Figure 5.** Friction force curves of the coatings.

To evaluate the surface energies of the coatings, force-distance measurements were performed with six different points on the surfaces. Collected force-distance curves were analyzed with SPIP software and average surface energies of the coatings were evaluated as shown in Figure 6. When looking the surface energies, it can be seen that AlTiN had the lowest surface energy (9.01 fJoule) as TiAlN (54.9 fJoule) and AlCrN (47.7 fJoule) had similar surface energy, where surface energy represents the work against two types of forces: first elastic forces, then adhesion forces (Bhushan, 2001; Israelachvili et al., 1994). Therefore, increase in adhesion between two sliding surfaces provides lower shear stress, and it increases the friction force (Mo et al., 2009; Yang and Komvopoulos, 2005; Spijker et al., 2013). Force-distance measurements presented lower surface energy and adhesion force for AlTiN surface.

The detected higher elastic modulus for the AlTiN was consistent with the surface energy findings. Furthermore, friction force increased linearly versus load deviation for the coatings, which presented that

Amonton's law was valid for coatings at nanoscale friction (Otsuki and Matsukawa, 2013), which results in lower COF than the TiAlN and AlCrN coatings.

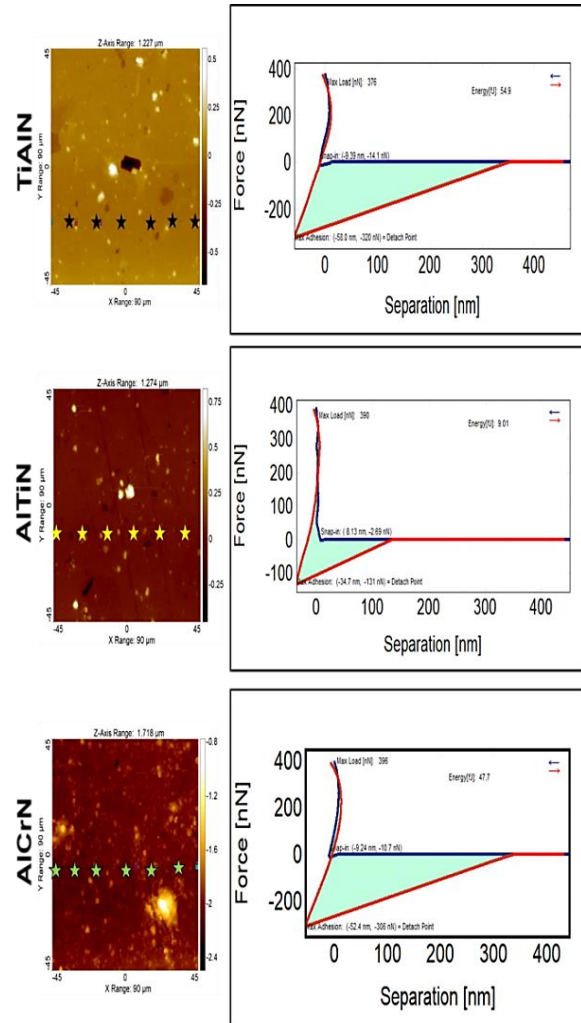


**Figure 6.** Force-distance curves and surface energy evolution of the TiAlN, AlTiN and AlCrN coatings.

#### 4. Conclusions

In this study, friction behavior of PVD deposited TiAlN, AlTiN and AlCrN multilayer coatings was investigated by FFM at the nanoscale. Based on the analysis results, the conclusions of this study can be summarized as follows:

- AlTiN showed approximately three times lower COF than the TiAlN and AlCrN coatings.
- Surface energy and adhesion forces between sliding surfaces can

characterize the friction force. AlTiN showed lower surface energy, which was the source of the lower COF than the other coatings.

- In this study, Amonton's law was valid for the COF evaluation at the nanoscale for the coatings, which is similar to macroscale. In addition to, macroscale COF evaluation will be done to compare nano and macroscale COF characteristics as a future work.

## 5. Acknowledgments

The author would like to thank the Koç University Surface Science and Technology Centre (KUYTAM) for SEM, nanoindentation analysis, and Mr. Onur Göz from Titanit company in Turkey supports for coatings.

## 6. References

- Asay, D.B., Kima, S.H. 2006. Direct force balance method for atomic force microscopy lateral force calibration. *Review of Scientific Instruments*, 77, 043903.
- Badisch, E., Roy, M. 2013. *Surface Engineering for Enhanced Performance against Wear*, Springer, London.
- Bhushan, B. 1999. *Principles and Applications of Tribology*.
- Bhushan, B. 2001. *Principles of tribology, Modern tribology handbook, Volume 1*, CRC Press, New York.
- Bhushan, B., Israelachvili, J.N., Landman, U. 1995. Nanotribology: friction, wear and lubrication at the atomic scale. *Nature*, 374, 607-616.
- Buckley, D.H. 1981. Surface effects in adhesion, friction, wear, and lubrication. *Tribology Series 5*, Elsevier, 247-249.
- Chu, S., Majumdar, A. 2012. Opportunities and challenges for a sustainable energy future. *Nature*, 488, 294-303.
- Holmberg, K., Andersson, P., Erdemir, A. 2012. Global energy consumption due to friction in passenger cars. *Tribology International*, 47, 221-234.
- Holscher, H., Schirmeisen, A., Schwarz, U. D. 2008. Principles of atomic friction: from sticking atoms to superlubric sliding. *Philosophical Transactions Series A, Mathematical, Physical, and Engineering Sciences*, 366, 1383-1404.
- Israelachvili, J.B., Chen, Y.L., Yoshizawa, H. 1994. Relationship between adhesion and friction forces. *Journal of Adhesion Science and Technology*, 8(11), 1231-1249.
- Lauda, P. 2007. Applications of thin coatings in automotive industry, *Journal of Achievements in Materials and Manufacturing Engineering*. 24, 51-56.
- Liew, W.Y.H., Jie, J.L.L., Yan, L.Y., Dayou, J., Sipaut, C.S., Madlan, M.F.B. 2013. Frictional and wear behavior of AlCrN, TiN, TiAlN single layer coatings, and TiAlN/AlCrN, AlN/TiN nano-multilayer coatings in dry sliding. *Procedia Engineering*, 68, 512-517.
- Manini, N., Mistura, G., Paolicelli, G., Tosatti, E., Vanossi, A. 2017. Current trends in the physics of nanoscale friction. *Advances in Physics: X*, 2 (3), 569-590.
- Mo, J.L., Zhu, M.H. 2009. Tribological oxidation behavior of PVD hard coatings. *Tribology International*, 42, 1758-1764.
- Mo, J.L., Zhu, M.H., Lei, B., Leng, Y.X., Huang, N. 2007. Comparison of

- tribological behaviors of AlCrN and TiAlN coatings-Deposited by physical vapor deposition. *Wear*, 263, 1423-1429.
- Mo, Y., Turner, K.T., Szlufarska, I. 2009. Friction laws at the nanoscale. *Nature*, 457, 1116-1119.
- Otsuki, M., Matsukawa, H. 2013. Systematic Breakdown of Amontons' Law of Friction for an Elastic Object Locally Obeying Amonton's Law. *Scientific Reports*, 3, 1586.
- Rosen, B.G., Ohlsson, R., Thomas, T.R. 1996. Wear of cylinder bore microtopography. *Wear*, 198, 271-279.
- Ruan, J.A., Bhushan, B. 1993. Atomic-Scale Friction Measurements Using Friction Force Microscopy: Part I—General Principles and New Measurement Techniques. *Journal of Tribology*, 116(2), 378-388.
- Sang, Y., Dubé, M., Grant, M. 2008. Dependence of friction on roughness, velocity, and temperature. *Physical Review E*, 77, 036123.
- Spijker, P., Anciaux, G., Molinari, J.F. 2013. Relations between roughness, temperature and dry sliding friction at the atomic scale. *Tribology International*, 59, 222–229.
- Stachowiak, G. W., Batchelor, A. W. 2000. *Engineering tribology*. Butterworth-Heinemann, 1-9.
- Svahn, F., Rudolphi, A.K., Wallén, E. 2003. The influence of surface roughness on friction and wear of machine element coatings. *Wear*, 254, 1092–1098.
- Xu, Q., Jensen, K.E., Boltyanskiy, R., Sarfati, R., Style, R.W., Dufresne, E.R. 2017. Direct measurement of strain-dependent solid surface stress. *Nature Communications*, 8(555), 1-6.
- Yang, J., Komvopoulos, K.A. 2005. Molecular Dynamics Analysis of Surface Interference and Tip Shape and Size Effects, on Atomic-Scale Friction. *Journal Tribology*, 127(3), 513-521.
- Zhang, S.W., Lan, H.Q. 2002. Developments in tribological research on ultrathin films. *Tribology International*, 35(5), 321-327.